

study by Doddoli et al.,<sup>7</sup> 20% in Downey et al.,<sup>8</sup> or 27% in Magdeleinat et al.<sup>9</sup> The postoperative mortality rate was 1.2% in this study, whereas Doddoli and associates reported postoperative mortality rates of 5.7% after lobectomy, 33.3% after bilobectomy, and 12.7% after pneumonectomy for resection of T3 diseases.<sup>7</sup> The lower mortality might have contributed to the relatively favorable prognosis in the current series.

The independent predictors of a poor prognosis after resection for locally advanced NSCLC were an incomplete resection, lymph node metastasis, and older age. Osaki et al. studied prognostic factors in patients with T4 disease, and reported that positive N2 lymph node metastasis and an incomplete resection were significantly predictive of a poorer prognosis, although their study included patients with malignant pleural effusion.<sup>4</sup> The current study was unique in light of the combination of T3 and T4 patients; however, the present results were very similar to other series. Therefore, these results should be helpful when considering the treatment of NSCLC invading neighboring organs.

Several phase II trials of preoperative concurrent chemoradiotherapy for stage III NSCLC indicated the feasibility of trimodality therapy. Ichinose et al. performed a phase II trial using induction chemoradiotherapy as an oral combination of uracil and tegafur plus cisplatin, and reported that 25 out of 27 patients (93%) showed partial response, with 22 patients undergoing tumor resection.<sup>10</sup> Their study revealed a 56% 3-year survival rate in all 27 patients and 67% 3-year survival rate in the 22 resected cases, with a 4% operative mortality rate. Stamatis et al. performed chemoradiotherapy using cisplatin+VP-16 following surgery for patients with stage IIIB NSCLC, and reported a 5-year survival rate of 26% in all cases and 43% survival in completely resected cases.<sup>11</sup> Grunenwald et al. studied chemoradiotherapy using cisplatin+5-fluorouracil+vinblastine followed surgery for patients with stage IIIB NSCLC, and reported 5-year survival rates of 19% in all cases and a survival of 42% in patients with no mediastinal lymph node involvement at the time of surgery and treatment with complete resection.<sup>12</sup> Further study is necessary to confirm the effectiveness of adjuvant therapy for patients with locally advanced lung carcinoma.

**Acknowledgments.** This work was supported in part by a Grant-in-aid for Scientific Research (C) Nos. 19591610 and 21591822 of the Japanese Ministry of Education, Culture, Sports, Science, and Technology.

## References

1. Riquet M, Lang-Lazdunski L, Le PB, Dujon A, Souilamas R, Danel C, et al. Characteristics and prognosis of resected T3 non-small cell lung cancer. *Ann Thorac Surg* 2002;73:253-8.
2. Burkhart HM, Allen MS, Nichols FC 3rd, Deschamps C, Miller DL, Trastek VF, et al. Management of en bloc resection for bronchogenic carcinoma with chest wall invasion. *J Thorac Cardiovasc Surg* 2002;123:670-5.
3. Martini N, Yellin A, Ginsberg RJ, Bains MS, Burt ME, McCormack PM, et al. Management of non-small cell lung cancer with direct mediastinal involvement. *Ann Thorac Surg* 1994;58:1447-51.
4. Osaki T, Sugio K, Hanagiri T, Takenoyama M, Yamashita T, Sugaya M, et al. Survival and prognostic factors of surgically resected T4 non-small cell lung cancer. *Ann Thorac Surg* 2003;75:1745-51.
5. Perrot M, Fadel E, Mussot S, de Palma A, Chapelier A, Dartevelle P. Resection of locally advanced (T4) non-small cell lung cancer with cardiopulmonary bypass. *Ann Thorac Surg* 2005;79:1691-6.
6. Naruke T, Tsuchiya R, Kondo H, Asamura H. Prognosis and survival after resection for bronchogenic carcinoma based on the 1997 TNM-staging classification: the Japanese experience. *Ann Thorac Surg* 2001;71:1759-64.
7. Doddoli C, D'Journo B, Le Pimpec-Barthes F, Dujon A, Foucault C, Thomas P, et al. Lung cancer invading the chest wall: a plea for en-bloc resection but the need for new treatment strategies. *Ann Thorac Surg* 2005;80:2032-40.
8. Downey RJ, Martini N, Rusch VW, Bains MS, Korst RJ, Ginsberg RJ. Extent of chest wall invasion and survival in patients with lung cancer. *Ann Thorac Surg* 1999;68:188-93.
9. Magdeleinat P, Alifano M, Benbrahem C, Spaggiari L, Porrello C, Puyo P, et al. Surgical treatment of lung cancer invading the chest wall: results and prognostic factors. *Ann Thorac Surg* 2001;71:1094-9.
10. Ichinose Y, Fukuyama Y, Asoh H, Ushijima C, Okamoto T, Ikeda J, et al. Induction chemoradiotherapy and surgical resection for selected stage IIIB non-small-cell lung cancer. *Ann Thorac Surg* 2003;76:1810-4.
11. Stamatis G, Eberhardt W, Stüben G, Bildat S, Dahler O, Hillejan L. Preoperative chemoradiotherapy and surgery for selected non-small cell lung cancer IIIB subgroups: long-term results. *Ann Thorac Surg* 1999;68:1144-9.
12. Grunenwald DH, André F, Le Péchoux C, Girard P, Lamer C, Laplanche A, et al. Benefit of surgery after chemoradiotherapy in stage IIIB (T4 and/or N3) non-small cell lung cancer. *J Thorac Cardiovasc Surg* 2001;122:796-802.



## Narrow band imaging with high-resolution bronchovideoscopy: A new approach for visualizing angiogenesis in squamous cell carcinoma of the lung

Kiyoshi Shibuya<sup>a,c,\*</sup>, Takahiro Nakajima<sup>a</sup>, Taiki Fujiwara<sup>a</sup>, Masako Chiyo<sup>a</sup>, Hidehisa Hoshino<sup>a</sup>, Yasumitsu Moriya<sup>a</sup>, Makoto Suzuki<sup>a</sup>, Kenzo Hiroshima<sup>b</sup>, Yukio Nakatani<sup>b</sup>, Ichiro Yoshino<sup>a</sup>

<sup>a</sup> Department of Thoracic Surgery, Graduate School of Medicine, Chiba University, 1-8-1 Inohana, Chuo-ku, Chiba 260-8670, Japan

<sup>b</sup> Department of Diagnostic Pathology, Graduate School of Medicine, Chiba University, 1-8-1 Inohana, Chuo-ku, Chiba 260-8670, Japan

<sup>c</sup> Department of Chest Surgery, Matsudo City Hospital, 4005 Kamihongo, Matsudo 271-8511, Japan

### ARTICLE INFO

#### Article history:

Received 18 February 2010

Received in revised form 21 April 2010

Accepted 25 April 2010

#### Keywords:

Narrow band imaging

High-resolution bronchovideoscopy

Angiogenesis

Multi-step carcinogenesis

Angiogenic squamous dysplasia

Squamous cell carcinoma

### ABSTRACT

**Objectives:** We investigated the ability of a high-resolution bronchovideoscopy system with narrow band imaging (NBI) to detect blood vessel structures in squamous cell carcinoma (SCC) of bronchi, as well as squamous dysplasia.

**Methods:** Seventy-nine patients with either abnormal sputum cytology or lung cancer were entered into the study. First, high-resolution bronchovideoscopy with white light was performed. Observations were repeated using NBI light to examine microvascular structures in the bronchial mucosa. Spectral features of the RGB (red/green/blue) sequential videoscope system were changed from a conventional RGB filter to the new NBI filter. The wavelength ranges of the NBI filter were: 400–430 nm (blue), 400–430 nm (green) and 520–560 nm (red).

**Results:** The following were clearly observed with NBI with high-resolution bronchovideoscopy: increased vessel growth and complex networks of tortuous vessels of various sizes, in squamous dysplasia; some dotted vessels, in addition to increased vessel growth and complex networks of tortuous vessels, in ASD; several dotted vessels and spiral or screw type tumor vessels of various sizes and grades, in SCC. Capillary blood vessel and/or tumor vessel mean diameters of ASD, CIS, microinvasive and invasive carcinoma were  $41.4 \pm 9.8 \mu\text{m}$ ,  $63.7 \pm 8.2 \mu\text{m}$ ,  $136.5 \pm 29.9 \mu\text{m}$  and  $259.4 \pm 29.6 \mu\text{m}$ , respectively. These results indicated a statistically significant increase of mean vessel diameters in the four groups ( $P < 0.0001$ ).

**Conclusion:** NBI with high-resolution bronchovideoscopy was useful for detecting the increased vessel growth and complex networks of tortuous vessels, dotted vessels and spiral or screw type tumor vessels of bronchial mucosa. This may enable detecting the onset of angiogenesis during multi-step carcinogenesis of the lung.

© 2010 Elsevier Ireland Ltd. All rights reserved.

### 1. Introduction

Narrow band imaging (NBI) is a new optical technology of modified white light using special blue and green light that can clearly visualize microvascular structures in the mucosal layer [1,2]. NBI is now classified as an image enhanced endoscopy (IEE) technology and is available to the entire field of endoscopy combined with conventional white light instruments [3,4]. The advantage of NBI over other techniques is its ability to enhance fine superficial microves-

sel patterns [5,6]. Since the development of NBI, some investigators have reported that this new technology can provide clear images of vascular structures in some organs especially the GI tract [7–17]. NBI may also allow for better detection of early preneoplastic and neoplastic mucosal lesions and may improve the effectiveness of endoscopic surveillance and screening. Moreover, in the field of bronchovideoscopy, we have also reported that high magnification bronchovideoscopy combined with NBI was useful for detecting capillary blood vessels in angiogenic squamous dysplasia (ASD) lesions [13]. Using high magnification bronchovideoscopy combined with NBI, increased vessel growth and complex networks of tortuous vessels, in addition to several dotted vessels, were identified in dysplastic mucosa or angiogenic dysplastic mucosa.

Angiogenesis that is essential for tumor growth was first recognized by Folkman [18,19]. In order to progress to a larger size, incipient neoplasia must develop angiogenic capabilities. Several studies investigating the multi-step model of carcinogenesis in

**Abbreviations:** NBI, narrow band imaging; RGB, red/green/blue; IEE, image enhanced endoscopy; ASD, angiogenic squamous dysplasia; CIS, carcinoma in situ.

\* Corresponding author at: Department of Chest Surgery, Matsudo City Hospital, 4005 Kamihongo, Matsudo 271-8511, Japan. Tel.: +81 47 363 2171;

fax: +81 47 363 2189.

E-mail address: [shibuya-ths@umin.ac.jp](mailto:shibuya-ths@umin.ac.jp) (K. Shibuya).

epithelial tumors have shown that angiogenesis is required, in addition to molecular changes [20]. An angiogenic switch appears to occur in pre-invasive lesions prior to invasive tumor formation in transgenic mouse models and human cancer pathogenesis studies [21,22]. However, except for a few studies, these studies were done on tissue sections retrospectively obtained from surgical or biopsied specimens. In vivo investigations to evaluate tumor angiogenesis during multi-step carcinogenesis is desirable for diagnostic efficacy.

In a previous study, we showed angiogenesis only in bronchial dysplastic lesions using high magnification bronchovideoscopy combined with NBI at sites of abnormal fluorescence established by fluorescence bronchoscopy [13]. In the present study, we investigated the ability of a high-resolution bronchovideoscopy system with NBI to detect and visualize blood vessel structures in squamous cell carcinoma of the bronchi, including carcinoma in situ (CIS), microinvasive carcinoma and invasive carcinoma, as well as dysplastic bronchial epithelium, including ASD lesions, without using fluorescence bronchoscopy.

## 2. Materials and methods

### 2.1. Narrow band imaging

The conventional RGB sequential videoscope system has a xenon lamp and rotation disk with 3 RGB optical filters. The rotation disk and monochrome CCD are synchronised and three band images are generated sequentially. Colour images can be synthesised using three band images with the video processor. Narrow band imaging, developed in conjunction with the Olympus Optical Corp., Tokyo, Japan, is a novel system that can be used to observe microvessel structure using a new narrow band filter on an RGB sequential videoscope system instead of the conventional RGB broadband filter [13]. In the conventional RGB sequential videoscope system, the image using 400–500 nm (blue) filter, which we termed the “B image”. It is most appropriate, by the principle of NBI, to choose 400–430 nm to observe capillaries on the surface and 520–560 nm for thicker blood vessels.

In the current study, wavelength ranges of the new NBI filter were 400–430 nm (blue), 400–430 nm (green), and 520–560 nm (red). In contrast, the wavelength ranges in the conventional RGB broadband filter were 400–500 nm (blue), 500–600 nm (green), and 600–700 nm (red). The main chromophore in the visible wavelength range in bronchial tissues is haemoglobin, which has a maximum absorptive wavelength near 415 nm, and is within the

wavelength range for NBI-blue and green (400–430 nm). When conventional RGB broadband light is delivered through an endoscope onto a tissue surface, some of the light is reflected from the tissue, some is scattered or absorbed within the tissue, and little light is detected to form an image on television monitors. However, narrow band light delivered onto the same surface shows less scattering and makes it possible to show clearer television monitor images [13].

There are two different types of video endoscopy system for the NBI technology. One is based on a monochrome CCD, in which colour separation is achieved through the use of a RGB optical filter within the light source unit. The second system is based on a colour CCD chip which has several tiny colour filters in each pixel. In this study, we used the former video endoscopy system. However, another investigator has used the latter video endoscopy system for the early lung cancer detection method.

### 2.2. High-resolution bronchovideoscopy

High-resolution bronchovideoscopy (BF-6C260, Olympus Optical Corp., Tokyo, Japan) was introduced in November 2003. Endovideoscopes with high CCD chips with 850K pixel density are referred to as high-resolution endovideoscopes. High-resolution bronchovideoscopy has an advanced, high-resolution CCD capable of capturing high quality images not possible before and ensures the highest quality in bronchovideoscope series in both normal and NBI images. While conventional white light bronchofiberscopy showed only increased redness and local swelling, high-resolution bronchovideoscope enabled visualization of the vascular networks with increased vessel growth and complex networks in the bronchial mucosa.

### 2.3. Study population and bronchoscopic procedures

Seventy-nine patients with sputum cytology specimens suspicious or positive for malignancy and lung cancer patients seen at the Department of Thoracic Surgery, Graduate School of Medicine, Chiba University in Chiba, from January 2005 to December 2007, were entered into the study. A mass screening of sputum cytological examinations was carried out to identify cases at high risk for lung cancer. The high risk group included patients 50 years or older with 30 or more pack-years of smoking, and those 40 years or older who had bloody sputum within the past 6 months. There were 75 males and 4 females ranging in age from 42 to 77 years (mean 66 years). Smoking history in pack-years ranged from 25 to 120 (mean

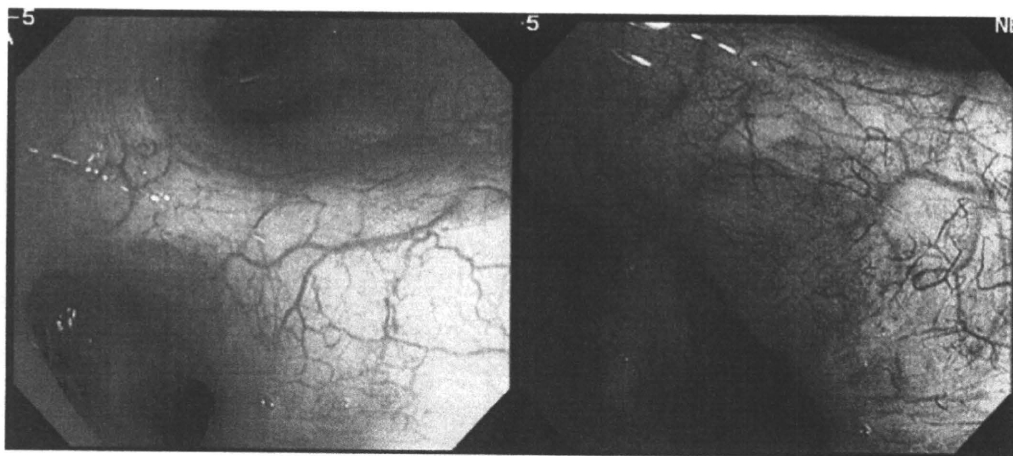


**Fig. 1.** High-resolution bronchovideoscopy combined with NBI of the bronchial mucosa. The high-resolution bronchovideoscopy system has an advanced, high-resolution CCD that is capable of capturing high quality images not possible before. Compared to conventional broadband images, NBI images provided more accurate images of various grades of microvessels. Lt, conventional white light image, Rt, NBI image.

54). Sixty-nine of the patients were current smokers and 10 were ex-smokers.

High-resolution bronchovideoscopy with white light was performed under local anaesthesia with sedation by intravenous midazolam injection and O<sub>2</sub> inhalation. Observations were repeated with NBI light to examine microvascular networks in the bronchial mucosa. The images could be changed from WL to NBI and vice versa with a touch of a switch. Both WL and NBI images could be synthesised using three band fusion images by a video processor.

Bronchial biopsy specimens for pathological examination were obtained from all abnormal areas examined. Images obtained by high-resolution bronchovideoscopy were examined and compared with pathological diagnoses from bronchial biopsy specimens. All participants provided written informed consent before enrolment into the study.

#### 2.4. High-resolution bronchovideoscopy combined with NBI of the bronchial mucosa

High-resolution bronchovideoscopy combined with NBI enabled the microvascular structures in the bronchial mucosa to be visualized more accurately. Typical high-resolution bronchoscopic findings from conventional RGB and NBI are shown in Fig. 1. Compared to conventional broadband images, NBI images provided more accurate images of various grades of microvessels. Thus, using our new NBI system, it was possible to discern microvessel

structures that could not be seen by means of conventional broadband systems.

#### 2.5. Evaluation of microvessel structures

Based on our previous classification and another field of endoscopic classification [7,13], lesions with vascular networks having a regular pattern were categorized as bronchitis; lesions with increased vessel growth and complex networks of tortuous vessels, as squamous dysplasia; lesions with several dotted vessels, in addition to increased vessel growth and complex networks of tortuous vessels, as ASD; lesions with only dotted vessels and small spiral or screw type tumor vessels, as CIS; and lesions with several dotted vessels and mid-large sized spiral or screw type tumor vessels, as microinvasive or invasive squamous cell carcinoma.

#### 2.6. Histopathological analysis

Biopsy specimens were fixed in 10% neutral formalin, embedded in paraffin, and stained with haematoxylin–eosin for histological study. Biopsy slides were first evaluated by a pathologist in our department, and then all slides were reviewed by expert pulmonary pathologists in our department (KH and YN). Bronchial squamous dysplasia and squamous cell carcinoma, including CIS and invasive carcinoma were diagnosed according to recent World Health Organization criteria.

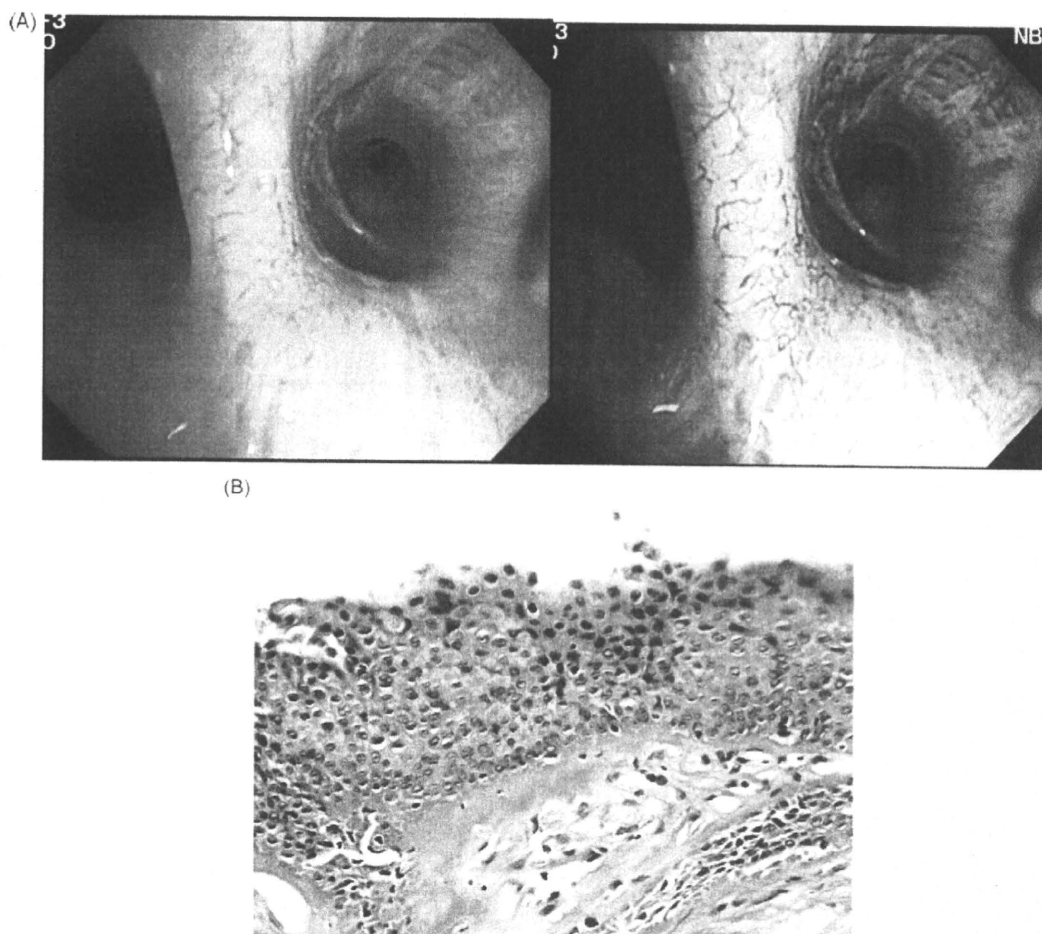


**Fig. 2.** (A) High-resolution bronchoscopic imaging with both WL and NBI of bronchial squamous dysplasia. Increased vessel growth and complex networks of tortuous vessels were observed by high-resolution bronchovideoscopy with NBI images. (B) Photomicrograph of bronchial squamous dysplasia. Pathological examination of the biopsy specimen showed squamous dysplasia.



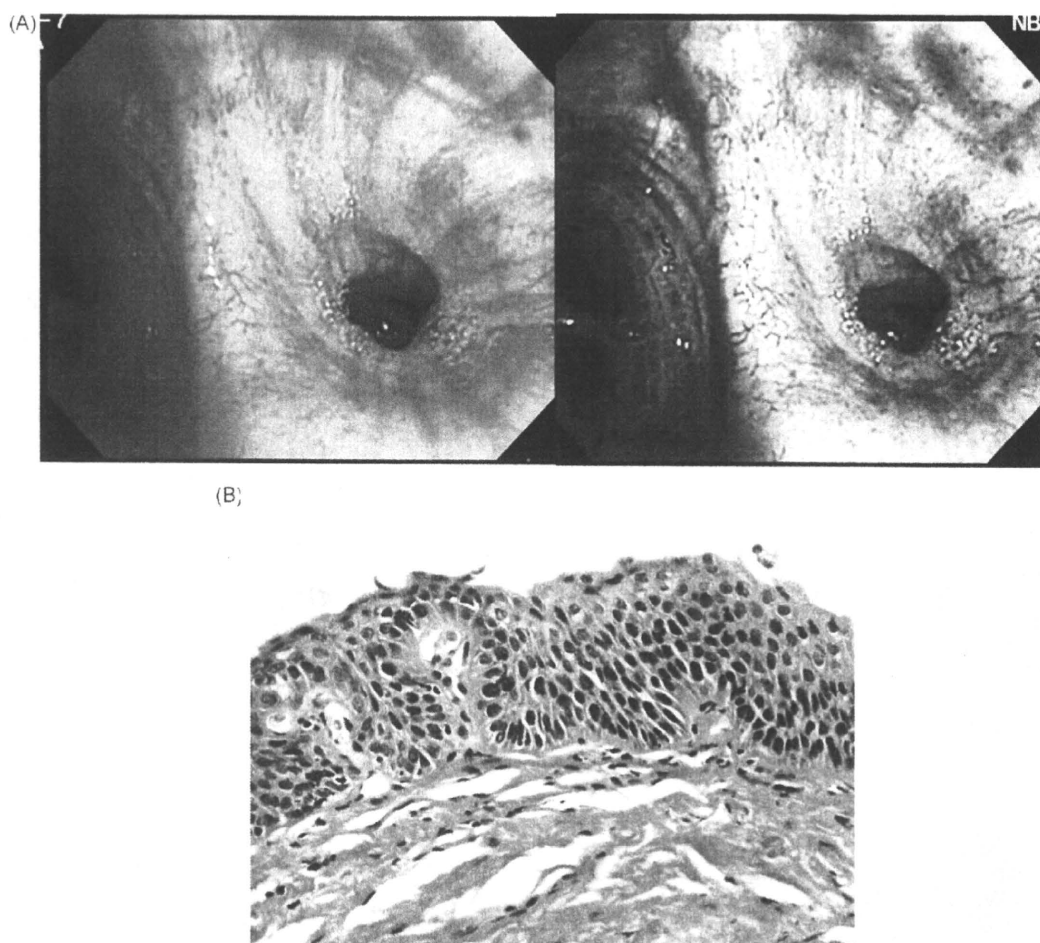


**Fig. 3.** (A) High-resolution bronchoscopic imaging with both WL and NBI of ASD. Several dotted vessels, in addition to increased vessel growth and complex networks of tortuous vessels, were more accurately observed by high-resolution bronchovideoscopy with NBI images. (B) Photomicrograph of ASD. Pathological examination of the biopsy specimen showed ASD. Collections of capillary-sized blood vessels closely juxtaposed to, and projecting into, dysplastic bronchial epithelium.

### 2.7. Calculation of diameters of capillary blood vessels and tumor vessels in biopsied specimens

Using an Image Cytometry Cell Analysis System (CAS 200; Becton Dickenson, San Jose, CA, USA) Micrometer Program, we calculated the diameter of the capillary blood vessels and tumor vessels in ASD, CIS, microinvasive carcinoma and invasive carcinoma identified by histology using a haematoxylin/eosin stained biopsy slide.

### 2.8. Statistical analysis

ANOVA was used to evaluate any significant differences between results, with  $P$  values  $\leq 0.05$  considered statistically significant. Statistical analysis was performed using the statistical software package Stat View (SAS Inc, Cary, NC, USA).

## 3. Results

### 3.1. Pathological diagnosis of biopsy specimens

Biopsy specimens from abnormal sites were diagnosed as 37 bronchial squamous dysplasias including 22 ASD, 5 CIS, 5 microinvasive carcinomas and 14 invasive squamous cell carcinomas. Two laryngeal carcinomas in situ and one laryngeal invasive carcinoma were also diagnosed in the same session.

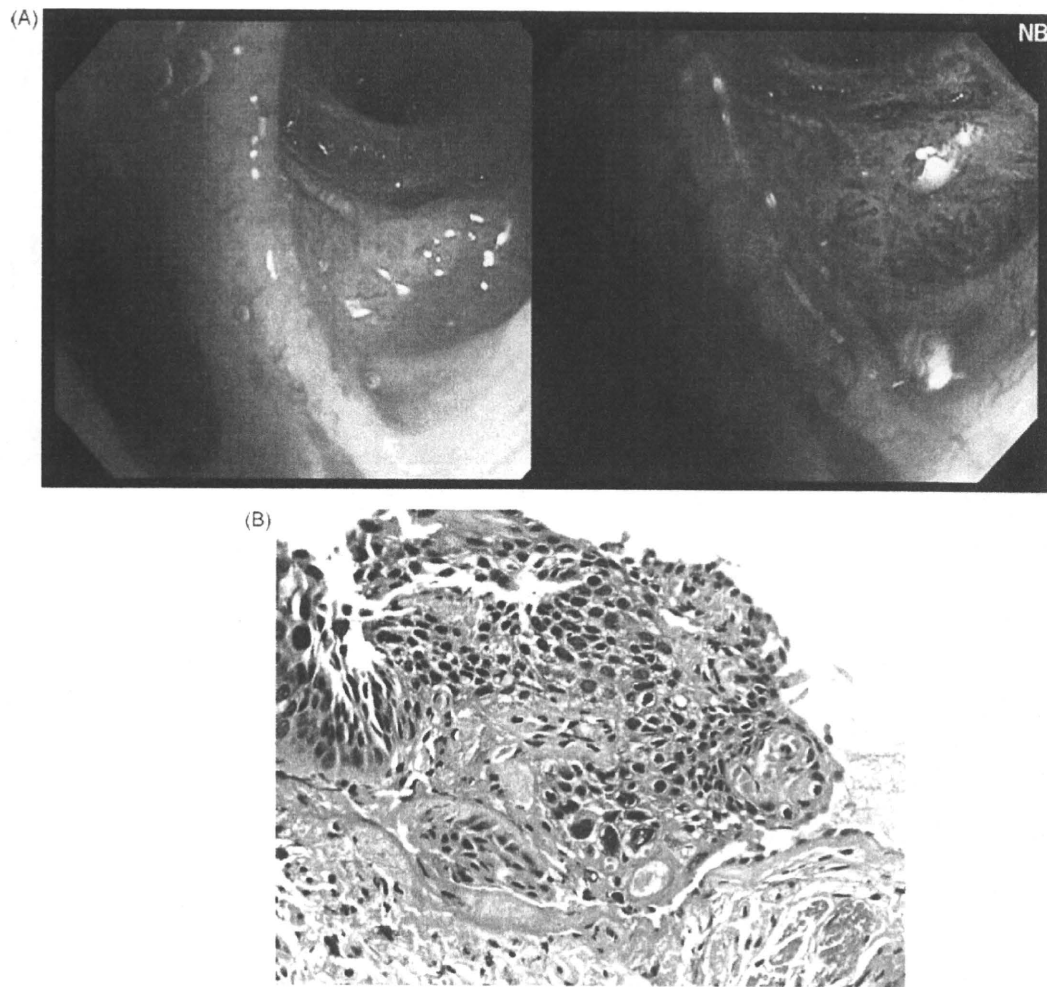
### 3.2. High-resolution bronchovideoscopic white light image and the corresponding NBI image

Fig. 2A shows high-resolution bronchoscopic findings with white light and NBI at the bifurcation of Rt B6 and the basal bronchus of a patient with sputum cytology suspicious for malignancy. Increased vessel growth and complex networks of tortuous vessels were observed by high-resolution bronchovideoscopy with NBI images. Pathological examination of the biopsy specimen showed squamous dysplasia (Fig. 2B).

Fig. 3A shows high-resolution bronchoscopic findings with white light and NBI at the bifurcation of Lt B6 and the basal bronchus of a patient with sputum cytology suspicious for malignancy. Several dotted vessels, in addition to increased vessel growth and complex networks of tortuous vessels, were more accurately observed by high-resolution bronchovideoscopy with NBI images. Pathological examination of the biopsy specimen showed ASD lesions (Fig. 3B).

Fig. 4A shows high-resolution bronchoscopic findings with white light and NBI at the entrance of Rt B10a of a patient with sputum cytology suspicious for malignancy. Several dotted vessels and small spiral or screw type tumor vessels in some grades were observed by high-resolution bronchovideoscopy with NBI. Pathological examination of the biopsy specimen showed squamous cell carcinoma in situ (Fig. 4B).

Fig. 5A shows high-resolution bronchoscopic findings with white light and NBI at the entrance of rt middle lobe bronchus.



**Fig. 4.** (A) High-resolution bronchoscopic imaging with both WL and NBI of CIS. Several dotted vessels and small spiral or screw type tumor vessels in some grades were observed by high-resolution bronchovideoscopy with a NBI images. (B) Photomicrograph of CIS. Pathological examination of the biopsy specimen showed squamous cell carcinoma in situ.

Several dotted vessels and spiral or screw type tumor vessels of various sizes and various grades were visible by high-resolution bronchovideoscopy with a conventional RGB broadband filter. NBI provided more accurate images of various grades of microvessel structures. Pathological examination of the biopsy specimen showed squamous cell carcinoma (Fig. 5B).

Fig. 6A shows high-resolution bronchoscopic findings with white light and NBI at the entrance of the upper lobe bronchus. Several dotted vessels and spiral or screw type tumor vessels of various sizes and grades, especially larger size, were visible by high-resolution bronchovideoscopy with a conventional RGB broadband filter. NBI provided more accurate images of various grades of microvessel structures. Pathological examination of the biopsy specimen showed squamous cell carcinoma (Fig. 6B).

### 3.3. Comparisons of microvessel diameters in ASD, CIS, microinvasive carcinoma and invasive carcinoma observed microscopically

Capillary blood vessel and tumor vessel diameters were compared between 11 ASD, 5 CIS, 5 microinvasive carcinomas and 10 invasive carcinomas calculated by an Image Cytometry (CAS 200) Cell Analysis System. Fig. 7 shows the mean vessel diameters. The mean vessel diameters were: ASD =  $41.4 \pm 9.8 \mu\text{m}$ ; carcinoma in situ =  $63.7 \pm 8.2 \mu\text{m}$ ; microinvasive carcinoma =  $136.5 \pm 29.9 \mu\text{m}$ ; and invasive carcinoma =  $259.4 \pm 29.6 \mu\text{m}$ . The diameters of the

capillary blood vessels and tumor vessels of invasive carcinoma were significantly larger compared with those of ASD, CIS and microinvasive carcinoma. The diameters of the capillary blood vessels and tumor vessels of microinvasive carcinoma were significantly larger compared with those of ASD and CIS. The diameters of the capillary blood vessels of CIS were significantly larger compared with those of ASD. These results indicate a statistically significant increase of mean vessel diameters in the four groups ( $P < 0.0001$ ) (Fig. 7).

### 3.4. Vessel morphology during lung cancer pathogenesis established by NBI imaging using high-resolution bronchovideoscope

The bronchial mucosal blood vessel structures in heavy smokers during multi-step carcinogenesis of squamous cell carcinoma, using NBI with high-resolution bronchovideoscopy, can be summarized as follows (Fig. 8). Increased vessel growth and complex networks of tortuous vessels of various sizes were observed with squamous dysplasia. Furthermore, some dotted vessels, in addition to increased vessel growth and complex networks of tortuous vessels, were visible with ASD lesions. With CIS, complex networks of tortuous vessels were not found, and only dotted vessels and small spiral or screw type tumor vessels were clearly observed. Several dotted vessels and spiral or screw type tumor vessels of various sizes and grades were visible in microinvasive to invasive lung can-

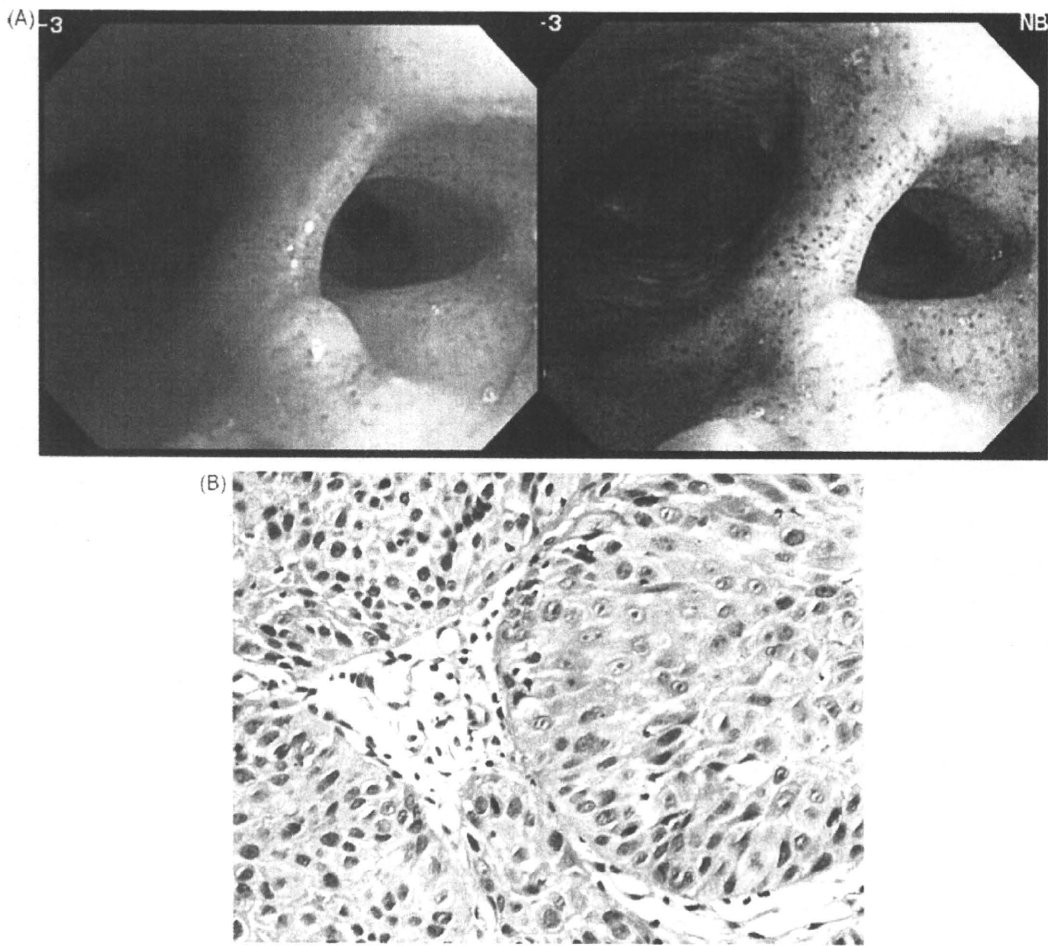


**Fig. 5.** (A) High-resolution bronchoscopic imaging with both WL and NBI of microinvasive squamous cell carcinoma. Several dotted vessels and spiral or screw type tumor vessels of various sizes and grades were visible by high-resolution bronchovideoscopy with a conventional RGB broadband filter. NBI images provided more accurate images of various grades of microvessel structures. (B) Photomicrograph of microinvasive squamous cell carcinoma. Pathological examination of the biopsy specimen showed squamous cell carcinoma.

cer patients. Dotted vessels and spiral or screw type tumor vessels were found to be thicker, and more distinct, in proportion to the severity of histological changes from ASD or CIS to microinvasive or invasive lung carcinoma.

#### 4. Discussion

NBI is now classified as an IEE technology, that can be divided into two categories, dye-based IEE and equipment-based IEE [4]. Optical and electronic technology have both been enabled in equipment-based IEE, which was applied to NBI, or spectral estimation technology and surface enhancement. NBI technologies have been well evaluated and established in the field of gastrointestinal endoscopy and applied to detailed inspections for pathological diagnosis. Recently, there are some reports concerning NBI in the field of bronchology [13–17]. Using NBI bronchovideoscopy, some researchers represent not only early detection of preneoplastic bronchial lesion but also the assessment of advanced lung cancer extension in routine bronchoscopy and airway vascularity after lung transplantation. However, the indication and utility of NBI bronchoscopy have not been well established.

In the present study, we used a method of high-resolution bronchovideoscopy combined with NBI for a group of heavy smokers at high risk for lung cancer and patients with lung cancer. Several dotted vessels and spiral or screw type tumor vessels of various sizes and grades were clearly observed in NBI images of

squamous cell carcinomas, which reflected the development from carcinoma in situ, microinvasive carcinoma and invasive carcinoma. In a previous study, we showed that bronchial mucosa microvascular networks could be distinctly observed in NBI-B1 images obtained using the NBI filter, which could not be observed using conventional RGB broadband filters, including conventional B images [13].

Of the three NBI filters (NBI-B1, NBI-B2 and NBI-G), microvascular networks, including dotted vessels, were most clearly detected with NBI-B1 wavelengths. Wavelength ranges of the NBI filter used in the previous study were B1: 400–430 nm; B2: 420–470 nm; and G: 560–590 nm. Based on both the original and our previous investigations, it was proven that more accurate vascular structure could be provided using the narrow band wavelength of 400–430 nm [1,13]. Therefore, the wavelengths in the new NBI filter would be used at 400–430 nm (blue), 400–430 nm (green) and 520–560 nm (red). The NBI fusion images (three filter combinations) were compared with WL images. The latest model of the NBI system has a simple button that can change the images from WL to NBI, and thus high-resolution bronchoscopic findings from conventional RGB and corresponding NBI could be easily obtained during the examination time.

With the aim of elucidating the blood vessel structures in squamous cell carcinoma of the bronchi, including CIS and microinvasive carcinoma, a high-resolution bronchovideoscopy system using NBI was used to make observations were made of the bronchial mucosa. Examinations of microvascular networks in the

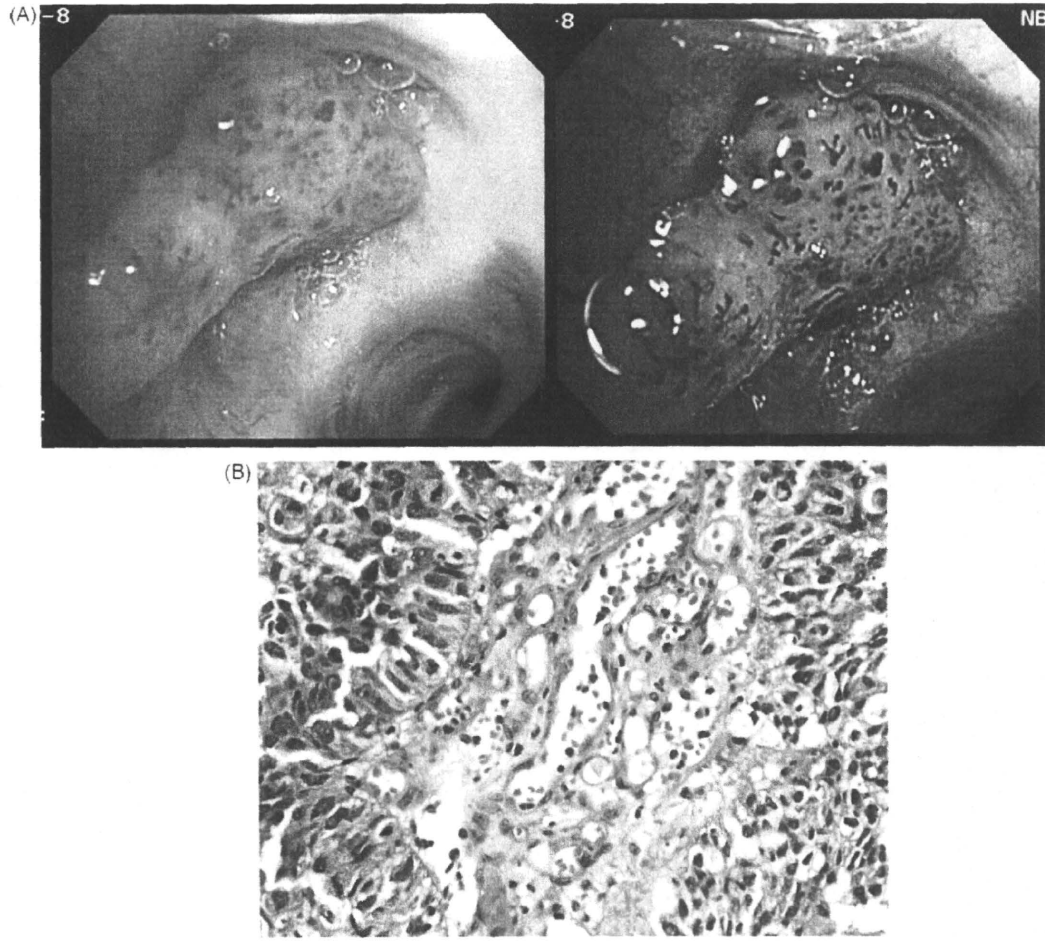


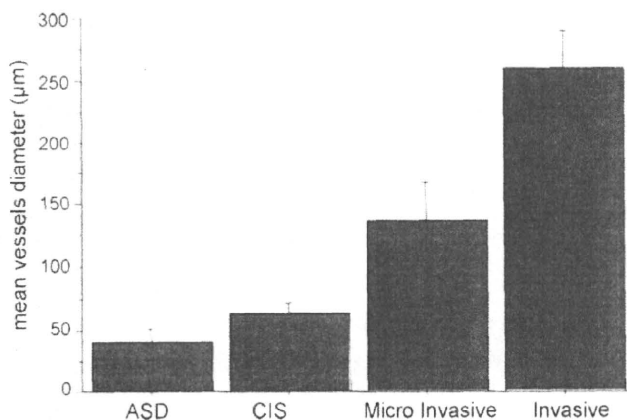
**Fig. 6.** (A) High-resolution bronchoscopic imaging with both WL and NBI of invasive squamous cell carcinoma. Several dotted vessels and spiral or screw type tumor vessels of various sizes and grades especially larger sizes, were visible by high-resolution bronchovideoscopy with a conventional RGB broadband filter. NBI images provided more accurate images of various grades of microvessel structures. (B) Photomicrograph of invasive squamous cell carcinoma. Pathological examination of the biopsy specimen showed squamous cell carcinoma.

bronchial mucosa using our system proved to be simple and effective. At sites of squamous cell carcinoma in situ, several dotted vessels and small spiral or screw type tumor vessels in some grades were observed; at sites of microinvasive squamous cell carcinoma,

several dotted vessels and spiral or screw type tumor vessels of various sizes and grades were observed; while at sites of invasive squamous cell carcinoma, several dotted vessels and spiral or screw type tumor vessels of various sizes and grades, especially larger sizes, were found.





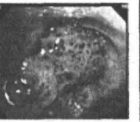
Our findings showed that many cases of squamous cell carcinoma had vascular patterns of dotted vessels and spiral or screw type tumor vessels of various sizes and grades. To obtain an objective evaluation of our findings, the diameters of the capillary blood vessels and tumor vessels in ASD, CIS, microinvasive carcinoma and invasive carcinoma were calculated using an Image Cytometry (CAS 200) Cell Analysis System. The diameters of the capillary blood vessels and tumor vessels of invasive carcinoma were significantly larger compared with those of ASD, CIS and microinvasive carcinoma. The diameters of the capillary blood vessels and tumor vessels of microinvasive carcinoma were significantly larger compared with those of ASD and CIS. The diameters of the capillary blood vessels of CIS were significantly larger compared with those of ASD. These results indicate a statistically significant increase of mean vessel diameters in the four groups.

Kumagai et al. reported that in the field of esophageal carcinoma, using high magnification endoscopy according to the caliber of intrapapillary capillary loops would improve the determination of depth of tumor invasion [23]. Using our new optical endoscopic image techniques, we may also be able to provide pre-treatment diagnosis of ASD or CIS, in addition to microinvasive carcinoma or invasive carcinoma of lung.



**Fig. 7.** Comparison of microvessel diameters in ASD, CIS, microinvasive carcinoma and invasive carcinoma observed microscopically. Calculation of diameters of capillary blood vessels and tumor vessels in biopsied specimens. Using an Image Cytometry Cell Analysis System (CAS 200; Becton Dickinson, San Jose, CA, USA) Micrometer Program, we calculated the diameters of the capillary blood vessels and tumor vessels in ASD, CIS, microinvasive carcinoma and invasive carcinoma. The mean vessels diameter of these four groups showed a statistically significant increase ( $P < 0.0001$ ).



	Squamous dysplasia	ASD	CIS	Micro invasive	Invasive
Tortuous vessel networks	+	+	–	–	–
Dotted vessels	–	+	+	++	+++
Spiral and screw type vessels	–	–	+	++	+++
					

**Fig. 8.** Vessel morphology during lung cancer pathogenesis established by NBI imaging using high-resolution bronchovideoscope. Summary of the bronchial mucosal blood vessel structures during multi-step carcinogenesis of squamous cell carcinoma using NBI with high-resolution bronchovideoscopy.

In a previous study, we showed angiogenesis only in bronchial dysplastic lesions using high magnification bronchovideoscopy combined with NBI at sites of abnormal fluorescence that were established by fluorescence bronchoscopy [13]. The high magnification bronchovideoscope was inserted into the tracheobronchial tree while observing progress using the fiber observation system for orientation until it could be confirmed that the tip had reached the target area. The tip was then brought close to the bronchial mucosa and the mucosa was observed at high magnification on a TV monitor. This procedure was difficult for reaching the abnormal area with only high magnification images. However, the high-resolution bronchovideoscopy system used in the present study is more practical because of the high quality images not possible before. We could easily determine which areas would be abnormal with the high-resolution bronchovideoscope, especially using NBI images.

In conclusion, NBI with high-resolution bronchovideoscopy was useful for detecting increased vessel growth and complex networks of tortuous vessels of various sizes, several dotted vessels and spiral or screw type tumor vessels of various sizes and grades in the bronchial mucosa. Capillary blood vessel and/or tumor vessel mean diameters for ASD, CIS, microinvasive carcinoma and invasive carcinoma showed statistically significant increases. This may enable detecting the onset of angiogenesis during multi-step carcinogenesis of the lung. NBI with high-resolution bronchovideoscopy enhances fine superficial microvessel patterns. This methodology could be applied to detailed inspections predictive of pathological diagnosis.

#### Conflict of interest

All authors have none declared.

#### Funding

Supported, in part, by Grant-in-Aid for Scientific Research (C) 18591541 from Japan Society for the Promotion of Science to Kiyoshi Shibuya.

#### Acknowledgements

We wish to thank K. Gono, T. Takigawa and S. Takehana (Olympus Optical Corp., Tokyo, Japan) for their technical assistance.

#### References

- [1] Gono K, Obi T, Yamaguchi M, Ohyama N, Machida H, Sano Y, et al. Appearance of enhanced tissue features in narrow-band endoscopic imaging. *J Biomed Opt* 2004;9:568–77.
- [2] Gono K, Igarashi M, Obi T, Yamaguchi M, Ohyama N. Multiple-discriminant analysis for light-scattering spectroscopy and imaging of two-layered tissue phantoms. *Opt Lett* 2004;29:971–3.
- [3] Tajiri H, Niwa H. Proposal for a consensus terminology in endoscopy: how should different endoscopic imaging techniques be grouped and defined? *Endoscopy* 2008;40:775–8.
- [4] Kaltenbach T, Sano Y, Friedland S, Soetikno R. American Gastroenterological Association (AGA) institute technology assessment on image-enhanced endoscopy. *Gastroenterology* 2008;134:327–40.
- [5] Curvers WL, Singh R, Song LM, Wolfsen HC, Ragunath K, Wang K, et al. Endoscopic tri-modal imaging for detection of early neoplasia in Barrett's oesophagus: a multi-centre feasibility study using high-resolution endoscopy, autofluorescence imaging and narrow band imaging incorporated in one endoscopy system. *Gut* 2008;57:167–72.
- [6] van den Broek FJ, Fockens P, van Eeden S, Reitsma JB, Hardwick JC, Stokkers PC, et al. Endoscopic tri-modal imaging for surveillance in ulcerative colitis: randomised comparison of high-resolution endoscopy and autofluorescence imaging for neoplasia detection; and evaluation of narrow-band imaging for classification of lesions. *Gut* 2008;57:1083–9.
- [7] Muto M, Nakane M, Katada C, Sano Y, Ohtsu A, Esumi H, et al. Squamous cell carcinoma in situ at oropharyngeal and hypopharyngeal mucosal sites. *Cancer* 2004;101:1375–81.
- [8] Watanabe A, Taniguchi M, Tsujie H, Hosokawa M, Fujita M, Sasaki S. The value of narrow band imaging for early detection of laryngeal cancer. *Eur Arch Otorhinolaryngol* 2009;266:1017–23.
- [9] Hamamoto Y, Endo T, Noshio K, Arimura Y, Sato M, Imai K. Usefulness of narrow-band imaging endoscopy for diagnosis of Barrett's esophagus. *J Gastroenterol* 2004;39:14–20.
- [10] East JE, Suzuki N, Stavrinidis M, Guenther T, Thomas HJ, Saunders BP. Narrow band imaging for colonoscopic surveillance in hereditary non-polyposis colorectal cancer. *Gut* 2008;57:65–70.
- [11] Sano Y, Ikematsu H, Fu KI, Emura F, Katagiri A, Horimatsu T, et al. Meshed capillary vessels by use of narrow-band imaging for differential diagnosis of small colorectal polyps. *Gastrointest Endosc* 2009;69:278–83.
- [12] Curvers WL, van den Broek FJ, Reitsma JB, Dekker E, Bergman JJ. Systematic review of narrow-band imaging for the detection and differentiation of abnormalities in the esophagus and stomach (with video). *Gastrointest Endosc* 2009;69:307–17.
- [13] Shibuya K, Hoshino H, Chiyo M, Iyoda A, Yoshida S, Sekine Y, et al. High magnification bronchovideoscopy combined with narrow band imaging could detect capillary loops of angiogenic squamous dysplasia in heavy smokers at high risk for lung cancer. *Thorax* 2003;58:989–95.
- [14] Vincent BD, Fraig M, Silvestri GA. A pilot study of narrow-band imaging compared to white light bronchoscopy for evaluation of normal airways and premalignant and malignant airways disease. *Chest* 2007;131:1794–9.
- [15] Herth FJ, Eberhardt R, Anantham D, Gompelmann D, Zakaria MW, Ernst A. Narrow-band imaging bronchoscopy increases the specificity of bronchoscopic early lung cancer detection. *J Thorac Oncol* 2009;10:60–5.
- [16] Zaric B, Becker HD, Perin B, Jovelic A, Stojanovic G, Ilic MD, et al. Narrow band imaging videobronchoscopy improves assessment of lung cancer

## Institutional report - Thoracic oncologic Surgical outcomes of newly categorized peripheral T3 non-small cell lung cancers: comparisons between chest wall invasion and large tumors (>7 cm)

Makoto Suzuki<sup>a,b,\*</sup>, Shigetoshi Yoshida<sup>a</sup>, Yasumitsu Moriya<sup>a</sup>, Hidehisa Hoshino<sup>a</sup>, Teruaki Mizobuchi<sup>a</sup>,  
Tatsuro Okamoto<sup>a</sup>, Ichiro Yoshino<sup>a</sup>

<sup>a</sup>Department of Thoracic Surgery, Graduate School of Medicine, Chiba University, Chiba, Japan

<sup>b</sup>Department of Thoracic Surgery, Kumamoto University Hospital, 1-1-1 Honjo, Kumamoto 860-8556, Japan

Received 12 May 2010; received in revised form 7 July 2010; accepted 9 July 2010

### Abstract

The prognosis for non-small cell lung cancer (NSCLC) with chest wall invasion can vary due to the heterogeneous nature of the cell population. Because NSCLC with large tumors (>7 cm) have been reclassified as T3, the applicability of the new designation must be evaluated. We reviewed 140 patients with chest wall T3 and 28 patients with T3 NSCLC with large tumors, but no chest wall invasion who underwent resection at our institution. Among chest wall T3 patients, elderly T3 patients ( $\geq 80$  years old) who died within 42 months, patients with either lymph node or pulmonary metastasis, or patients with a large tumor (>7 cm) had poorer prognoses than those who had not. The survival rates for cases with chest wall T3 and cases with a large tumor without chest wall invasion were not significantly different. NSCLC patients with chest wall T3 with lymph node, or pulmonary metastasis, or with a large tumor should be considered for further multimodal treatment with or without resection to enhance their survival time. Elderly patients with chest wall invasion may not be good candidates for resection. A large tumor is so aggressive that re-classification of large tumor cases as T3 is suitable.

© 2010 Published by European Association for Cardio-Thoracic Surgery. All rights reserved.

**Keywords:** Non-small cell lung cancer; Chest wall invasion; Stage; Prognosis

### 1. Introduction

Prognostic factors for T3 non-small cell lung cancer (NSCLC) with chest wall invasion have been reported [1–3]. The incompleteness of a resection and the presence of lymph node metastases are major prognostic factors for this disease [4, 5]. The efficacy of adjuvant treatment before or after surgery for chest wall invasion remains controversial, due to the heterogeneous population of T3 stage chest wall or lack of appropriate multimodal management for these cases [6, 7]. Therefore, clarification of the prognostic factors is important for establishing appropriate multimodal management of these patients based on subgrouping.

Chest wall invasion by NSCLC implies an apparent high permeability because it invades both the visceral and parietal pleura, and even muscle and bone [8]. In contrast, the potential infiltrating capability of large tumors (>7 cm) without chest wall invasion remains unknown. The seventh edition of TNM classification has categorized large tumors (>7 cm) as T3 [9], but the validity of this change requires further evaluation.

The aim of this study is to identify prognostic factors that may impact the long-term outcomes of patients with NSCLC invasion of the chest wall, and to compare their prognoses with cases with large tumors but without chest wall invasion.

### 2. Patients and methods

Between January 1990 and December 2007, 1623 NSCLC patients underwent curative resection at Chiba University Hospital, Chiba, Japan; 140 cases had chest wall invasion and 28 cases had a large tumor (>7 cm) without chest wall invasion. Wedge resections or sublobar resections were preferred for patients with severe respiratory function impairment. Because one aim was to compare the prognoses in the presence of large tumors, which are categorized as T3 in the TNM staging system outlined in the seventh edition of the American Joint Committee on Cancer (AJCC) Staging Manual, patients categorized as T3 due to invasion of the diaphragm, the mediastinal pleura, and the pericardium were included as one group. As a result, three patients (one case with invasion of the diaphragm, one with mediastinal pleura, and one with the pericardium) were included as chest wall T3. As for chest wall T3, en

\*Corresponding author. Tel.: +81-96-373-5533; fax: +81-96-373-5532.  
E-mail address: smakoto@kumamoto-u.ac.jp (M. Suzuki).

Table 1. Clinical characteristics of chest wall T3 and large (&gt;7 cm) non-small cell lung cancer patients

Clinical factors	Chest wall invasion (+)			Chest wall invasion (-) >7 cm
	≤7 cm	>7 cm	Total	
Gender				
Male	103	18	121	23
Female	16	3	19	5
Age, years				
<65	50	9	59	13
≤65, >75	49	10	59	10
≤75, >80	17	1	18	4
≤80	3	1	4	1
Smoking				
Smoker	101	19	120	23
Never smoker	18	2	20	5
Histology				
Adenocarcinoma	63	9	72	14
Squamous cell carcinoma	49	9	58	11
Others	7	3	10	3
Perioperative				
Treatment	10	3	13	3
None	109	18	127	25
Surgery				
Wedge/segmentectomy	3	0	3	2
Lobectomy	91	16	107	22
Bi-lobectomy	11	2	13	2
Pneumonectomy	14	3	17	2
Tumor size				
≤7 cm	119	0	119	0
>7 cm	0	21	21	28
Lymph node				
Metastasis (-)	66	13	79	20
Metastasis (+)	53	8	61	8
Pulmonary				
Metastasis (-)	105	20	125	28
Metastasis (+)	14	1	15	0
Sixth pTNM				
Stage IB	0	0	0	19
Stage IIB	61	12	73	4
Stage IIIA	44	8	52	5
Stage IIIB	14	1	15	0
Seventh pTNM				
Stage IIB	66	13	79	20
Stage IIIA	53	8	61	8

pTNM, pathologic TNM.

bloc resection and quick pathologic examination, if necessary, were performed to remove any residual tumor cells at the surgical margin. Pathological staging was determined according to the sixth (previous) [10] and seventh (current) editions of TNM classifications [9].

Survival was calculated from the date of surgery until death or the date of last follow-up. Survival curves were calculated using the Kaplan–Meier method, and comparisons were made using a log-rank test. Multivariate analyses used a Cox proportional hazards regression model to identify candidate factors for survival prediction. In each analysis, significance was set at  $P < 0.05$ .

### 3. Results

The patients' clinical features are shown in Table 1. The distributions of host, treatment, and tumor factors were not significantly different among the three categories: tumors ≤7 cm with chest wall invasion, tumors >7 cm

with chest invasion, and tumors >7 cm without chest wall invasion. All of the cases previously staged as IIIB were due to pulmonary metastasis in the same lobe. Thirteen patients received adjuvant treatment (chemotherapy or radiotherapy) before or after surgery. Incomplete resection was performed for five cases, for which quick examination was not performed during surgery. All patients received post-radiotherapy. Among them, two patients died due to distant metastasis, but three survived without recurrence. Three patients died of surgery-related complications. One patient died due to acute myocardial infarction 10 days after surgery. Two patients died within 48 days; one because of a bronchial fistula and the other because of acute respiratory dysfunction. The average follow-up was 49.3 months (range 1–207 months).

The effect of age on prognosis was analyzed by dividing the cases with chest wall invasion ( $n=140$ ) into four categories: <65 years of age; ≥65 years but <75 years; ≥75 years but <80 years; and ≥80 years (Fig. 1a). The first three groups showed similar prognoses, but the prognosis for the group ≥80 years old was very poor. Therefore, the cases were re-divided into two categories: <80 years and ≥80 years (Fig. 1b). In the <80 years subgroup, the five-year survival rate was 42.9% while all members in the ≥80 years subgroup died within 42 months due to recurrence ( $P=0.018$ ). Patients with lymph node metastasis had a five-year survival rate of 26.5%, while patients without lymph node metastasis had a rate of 53.3% ( $P=0.004$ , Fig. 1c). Patients with pulmonary metastasis had a five-year survival rate of 6.7%, while patients without pulmonary metastasis had a five-year survival rate of 46.4% ( $P=0.001$ , Fig. 1d).

Survival was also analyzed using previous and current TNM staging systems. Using the criteria for previous classification (sixth edition), the five-year survival rate was 33.5% for patients diagnosed as stage IIIA, 55.3% as stage IIB ( $P=0.044$ ), and 6.7% as stage IIIB ( $P=0.054$ , Fig. 1e). The five-year survival rate was 53.3% for patients in current stage IIB and 26.5% in stage IIIA ( $P=0.004$ , Fig. 1f). Interestingly, the difference between stage IIB and IIIA for the chest wall invasion cases, according to the current TNM staging system, is the presence of lymph node metastasis (N1 or N2). Thus, the results in Fig. 1c (lymph node metastasis) and Fig. 1f (current TNM staging) were identical.

The independent prognostic values of co-variables were tested using a Cox proportional hazard model (Table 2). Based on this analysis, age, lymph node metastasis, pulmonary metastasis, tumor size, previous staging, and current staging were all independent prognostic factors.

Next, we compared the prognoses of patients with chest wall invasion with those with large tumors without chest wall invasion. The five-year survival rate was 41.5% for patients with chest wall invasion, and 59.0% for patients with large tumors without chest wall invasion ( $P=0.28$ , Fig. 2a). Also, we compared these two categories without lymph node metastasis cases to avoid the influence of lymph node metastasis. The five-year survival rate was 52.1% for patients with chest wall invasion and without lymph node metastasis, and 72.1% for patients with large

tumors without either chest wall invasion or lymph node metastasis ( $P=0.34$ , Fig. 2b). However, when patients were divided into three categories, the five-year survival rate for patients with chest wall invasion was 27.2% when a large tumor was present versus 44.2% without a large tumor ( $P=0.054$ ), and 59.0% for patients with a large tumor but without chest wall invasion ( $P=0.047$  when compared with patients with a large tumor and chest wall invasion, Fig. 2c).

#### 4. Discussion

Many factors can compromise the long-term survival of patients with chest wall invasion T3 NSCLC. Lymph node metastasis has been a common prognostic factor for patients with chest wall invasion, as reflected in this study. Some authors have questioned whether surgery is of any benefit in this subset of patients [4, 11]. Mediastinoscopy is generally indicated to exclude the involvement of mediastinal lymph node metastasis [11]. Recent advances in assessing lymph node metastasis using endobronchial ultrasound-guided needle aspiration clarifies lymph node status before any treatment for lung cancer is initiated [12]. This technology helps with deciding whether surgery is appropriate for cases with chest wall invasion or if other modalities are indicated.

Table 2. Cox proportional hazards regression models for chest wall T3 non-small cell lung cancer

Co-variate	Factor comparisons	Hazard ratio	95% Confidence interval	P-value
Age, years	<80/≥80	4.17	1.48–11.7	0.007
Gender	Female/male	0.90	0.49–1.67	0.74
Lymph node	Metastasis (-)/(+)	1.83	1.17–2.87	0.008
Pulmonary	Metastasis (-)/(+)	2.69	1.45–4.98	0.002
Tumor size, cm	≤7/>7	2.27	1.27–4.07	0.006
Age, years	<80/≥80	3.69	1.33–10.30	0.01
Gender	Female/male	0.88	0.47–1.62	0.68
6th pTNM	Stage IIB			0.002
	Stage IIIA	1.61	0.996–2.60	0.052
	Stage IIIB	3.17	1.67–6.04	0.0004
Age, years	<80/≥80	3.33	1.20–3.23	0.021
Gender	Female/male	0.79	0.43–1.45	0.45
7th pTNM	Stage IIB/IIIA	1.63	1.05–2.54	0.029

pTNM, pathologic TNM.

Pulmonary metastasis in the same lobe was also a poor prognostic factor in this group. Although pulmonary metastasis in the same lobe has been down-staged to T3 from T4 in the current TNM staging, patients with the co-existence of two T factors (chest wall invasion and pulmonary metastasis) should be treated carefully.

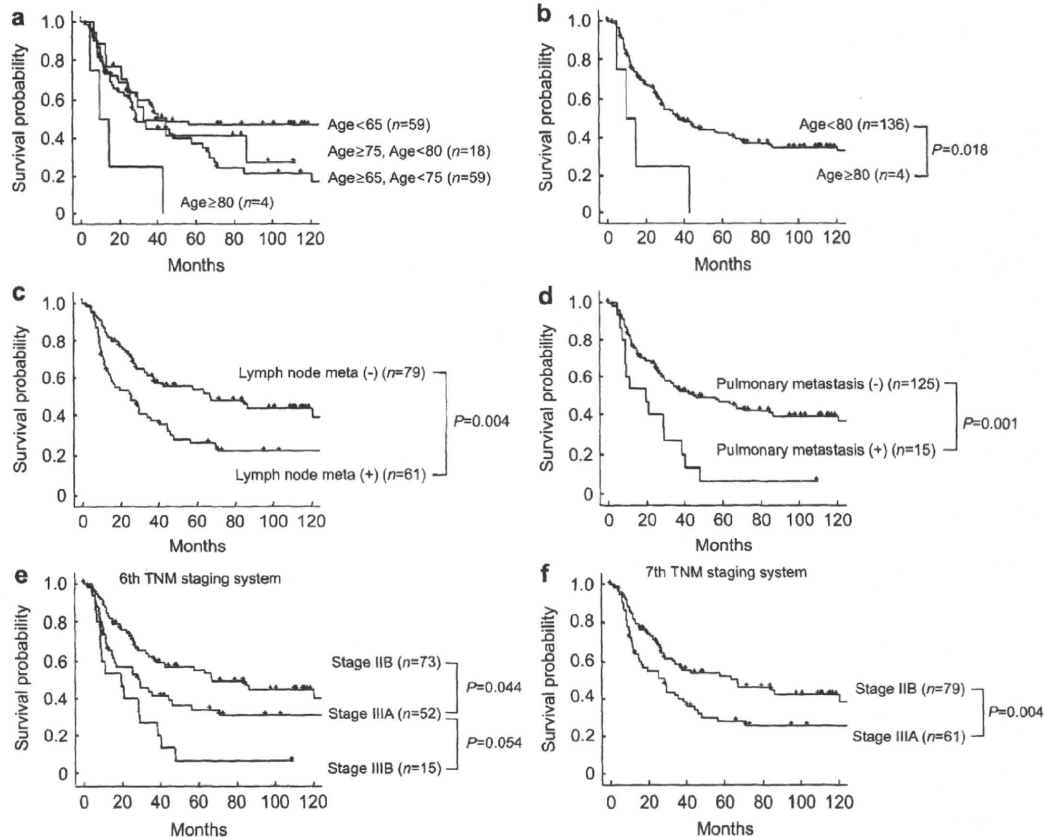


Fig. 1. Survival curves based on age, categorized into four (a), or two groups (b), lymph node status (c), pulmonary metastasis (d), sixth edition TNM staging (e), and seventh edition TNM staging (f). (c) and (f) are essentially the same because the differences in stages IIB and IIIA in the current revision are all due to lymph node metastasis, which is N1 or N2 in our cases.



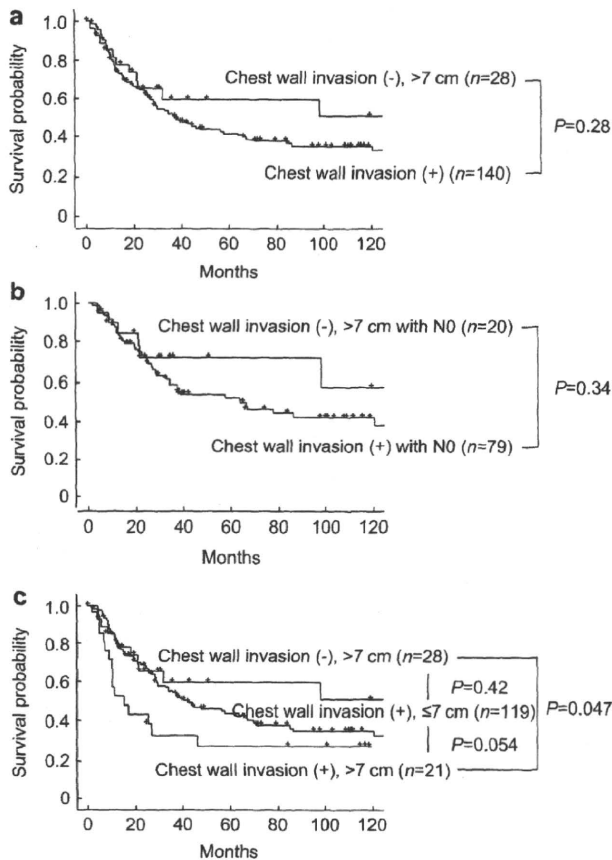


Fig. 2. Survival curves for chest wall T3 and large (>7 cm) NSCLC (a), those without lymph node metastasis (b), and chest wall T3 (<7 cm), chest wall T3 (>7 cm), and large tumor (>7 cm) NSCLC (c). NSCLC, non-small cell lung cancer.

This study also demonstrated the prognostic significance of advanced age ( $\geq 80$  years old). The current strategy for older patients with NSCLC is based on the premise that surgery is most effective only in the early stages of the disease [13, 14]. Based on our results, very elderly NSCLC patients ( $\geq 80$  years old) with chest wall invasion may not be surgical candidates.

Incomplete resection has also been reported as a factor for poorer prognosis [8, 11]. However, in this study, only five cases (4%) were positive-surgical margined with tumor cells and all received post-operative radiotherapy. The two deaths that occurred did not achieve statistical significance by a log-rank test ( $P=0.48$ ). The low frequency of incomplete resections and post-operative radiotherapy did not allow for the clarification of the impact of these procedures on patient survival in this study.

The prognostic significance of the depth of chest wall invasion remains controversial [6, 8, 15]. Because one aim of this study was to compare the utility of the current TNM staging, especially with the involvement of large tumors, we did not analyze the depth of tumor infiltration into the chest wall, which was not reflected in both the previous and current TNM staging criteria. However, T3 is currently sub-divided into T3a, T3b, and T3c according to the degree

of chest wall invasion. Although they are all T3, these factors must be considered separately in future analyses.

Some reports have discussed the utility of induction or adjuvant therapy for cases with chest wall invasion [7]. In our group, probably because of the small number of cases with adjuvant therapy ( $n=13$ ), we did not demonstrate the efficacy of adjuvant therapy for prognosis. However, this category should be evaluated further, especially for cases with lymph node or pulmonary metastasis.

By comparison with patients who had a large tumor without chest wall invasion, the survival of patients with chest wall invasion and cases with a large tumor without chest wall invasion were not significantly different. Therefore, categorizing large tumors as T3 may be suitable. However, if the tumor was both large and invasive, the co-existence of two T factors yielded a poorer prognosis than when only a single T factor was present (Fig. 2c).

Cases of chest wall invasion with pulmonary metastasis or with a large tumor (>7 cm) had poorer prognoses. These are not considered up-staging factors, while lymph node metastasis is considered up-staging. In the case of chest wall invasion, the frequencies of pulmonary metastasis and large tumors were relatively low: 8.6% (12/140) and 15% (21/140), respectively, compared with the frequency of lymph node metastasis (44%; 61/140). We should note that small sub-groups in the cases with chest wall invasion showed poorer prognoses, which was not reflected in TNM staging.

In conclusion, our study demonstrates several particular features of NSCLC with chest wall invasion. Pulmonary metastasis or a large tumor (>7 cm) that are not reflected in TNM staging, or lymph node metastasis that is reflected in TNM staging, had a disastrous impact on patient survival. In those cases, multimodal treatment with or without resection may be considered to prolong survival. Elderly patients ( $\geq 80$  years old) may not be good candidates for resection. Re-classification of large tumors as T3 may be suitable when compared with the prognosis of chest wall T3 tumors, although both large tumors and chest wall T3 had the worst prognoses among chest wall T3 ( $\leq 7$  cm), chest wall T3 (>7 cm), and large tumor T3 (>7 cm) without chest wall invasion groups.

## References

- [1] Stoelben E, Ludwig C. Chest wall resection for lung cancer: indications and techniques. *Eur J Cardiothorac Surg* 2009;35:450–456.
- [2] Mineo TC, Ambrogio V, Pompeo E, Baldi A. Immunohistochemistry-detected microscopic tumor spread affects outcome in en-bloc resection for T3-chest wall lung cancer. *Eur J Cardiothorac Surg* 2007;31:1120–1124.
- [3] Martin-Ucar AE, Nicum R, Oey I, Edwards JG, Waller DA. En-bloc chest wall and lung resection for non-small cell lung cancer. Predictors of 60-day non-cancer related mortality. *Eur J Cardiothorac Surg* 2003;23:859–864.
- [4] Doddoli C, D'Journo B, Le Pimpec-Barthes F, Dujon A, Foucault C, Thomas P, Riquet M. Lung cancer invading the chest wall: a plea for en-bloc resection but the need for new treatment strategies. *Ann Thorac Surg* 2005;80:2032–2040.
- [5] DiPerna CA, Wood DE. Surgical management of T3 and T4 lung cancer. *Clin Cancer Res* 2005;11:5038s–5044s.
- [6] Matsuoka H, Nishio W, Okada M, Sakamoto T, Yoshimura M, Tsubota N. Resection of chest wall invasion in patients with non-small cell lung cancer. *Eur J Cardiothorac Surg* 2004;26:1200–1204.

- [7] Voltolini L, Rapicetta C, Luzzi L, Ghiribelli C, Ligabue T, Paladini P, Gotti G. Lung cancer with chest wall involvement: predictive factors of long-term survival after surgical resection. *Lung Cancer* 2006;52:359–364.
- [8] Lin YT, Hsu PK, Hsu HS, Huang CS, Wang LS, Huang BS, Hsu WH, Huang MH. En bloc resection for lung cancer with chest wall invasion. *J Chin Med Assoc* 2006;69:157–161.
- [9] Goldstraw P, Crowley J, Chansky K, Giroux DJ, Groome PA, Rami-Porta R, Postmus PE, Rusch V, Sobin L. The IASLC Lung Cancer Staging Project: proposals for the revision of the TNM stage groupings in the forthcoming (seventh) edition of the TNM classification of malignant tumours. *J Thorac Oncol* 2007;2:706–714.
- [10] Mountain CF. Revisions in the international system for staging lung cancer. *Chest* 1997;111:1710–1717.
- [11] Allen MS. Chest wall resection and reconstruction for lung cancer. *Thorac Surg Clin* 2004;14:211–216.
- [12] Yasufuku K, Nakajima T, Fujiwara T, Chiyo M, Iyoda A, Yoshida S, Suzuki M, Sekine Y, Shibuya K, Yoshino I. Role of endobronchial ultrasound-guided transbronchial needle aspiration in the management of lung cancer. *Gen Thorac Cardiovasc Surg* 2008;56:268–276.
- [13] Suemitsu R, Takeo S, Hamatake M, Yoshino J, Motoyama M, Tanaka H. The perioperative complications for elderly patients with lung cancer associated with a pulmonary resection under general anesthesia. *J Thorac Oncol* 2009;4:193–197.
- [14] Suemitsu R, Yamaguchi M, Takeo S, Ondo K, Ueda H, Yoshino I, Maehara Y. Favorable surgical results for patients with nonsmall cell lung cancer over 80 years old: a multicenter survey. *Ann Thorac Cardiovasc Surg* 2008;14:154–160.
- [15] Magdeleinat P, Alifano M, Benbrahem C, Spaggiari L, Porrello C, Puyo P, Levasseur P, Regnard JF. Surgical treatment of lung cancer invading the chest wall: results and prognostic factors. *Ann Thorac Surg* 2001;71:1094–1099.

## Diagnostic yield of preoperative computed tomography imaging and the importance of a clinical decision for lung cancer surgery

Shuichi Sato, MD · Teruaki Koike, MD  
Yasushi Yamato, MD · Katsuo Yoshiya, MD  
Nozomu Motono, MD · Mariko Takeshige, MD  
Naoya Koizumi, MD · Keiichi Homma, MD, PhD  
Hiroko Tsukada, MD · Akira Yokoyama, MD

Received: 22 November 2009 / Accepted: 11 February 2010  
© The Japanese Association for Thoracic Surgery 2010

### Abstract

**Purpose.** This study aimed to evaluate the diagnostic yield of preoperative computed tomography (CT) imaging and the validity of surgical intervention based on the clinical decision to perform surgery for lung cancer or suspected lung cancer.

**Methods.** We retrospectively evaluated 1755 patients who had undergone pulmonary resection for lung cancer or suspected lung cancer. CT scans were performed on all patients. Surgical intervention to diagnose and treat was based on a medical staff conference evaluation for the suspected lung cancer patients who were pathologically undiagnosed. We evaluated the relation between resected specimens and preoperative CT imaging in detail.

**Results.** A total of 1289 patients were diagnosed with lung cancer by preoperative pathology examination; another 466 were not pathologically diagnosed preop-

eratively. Among the 1289 patients preoperatively diagnosed with lung cancer, the diagnoses were confirmed postoperatively in 1282. Among the 466 patients preoperatively undiagnosed, 435 were definitively diagnosed with lung cancer, and there were 383 p-stage I disease patients. There were 38 noncancerous patients who underwent surgery with a diagnosis of confirmed or suspected lung cancer. Among the 1755 patients who underwent surgery, 1717 were pathologically confirmed with lung cancer, and the diagnostic yield of preoperative CT imaging was 97.8%. Among the 466 patients who were preoperatively undiagnosed, 435 were compatible with the predicted findings of lung cancer.

**Conclusion.** Diagnostic yields of preoperative CT imaging based on clinical evaluation are sufficiently reliable. Diagnostic surgical intervention was acceptable when the clinical probability of malignancy was high and the malignancy was pathologically undiagnosed.

**Key words** Preoperative diagnosis · Computed tomography imaging · Clinical decision · Surgical intervention

### Introduction

Lung cancer is a major cause of cancer-related death in Japan. It is the leading cause of cancer-related deaths in men, and the second leading cause, after colorectal cancer, in women. In 2007, the annual report of the Ministry of Health, Labour, and Welfare documented approximately 336 000 cancer-related deaths, of which 65 000 were due to lung cancer.<sup>1</sup>

Due to recent advances in diagnostic modalities, especially high-resolution computed tomography (HRCT)

---

S. Sato · T. Koike (✉) · Y. Yamato · K. Yoshiya · N. Motono · M. Takeshige  
Division of Chest Surgery, Niigata Cancer Center Hospital,  
2-15-3 Kawagishi-cho, Niigata 951-8566, Japan  
Tel. +81-25-266-5111; Fax +81-25-233-3649  
e-mail: koike@niigata-cc.jp

N. Koizumi  
Division of Diagnostic Radiology, Niigata Cancer Center  
Hospital, Niigata, Japan

K. Homma  
Division of Pathology, Niigata Cancer Center Hospital, Niigata,  
Japan

H. Tsukada · A. Yokoyama  
Division of Pulmonology, Niigata Cancer Center Hospital,  
Niigata, Japan

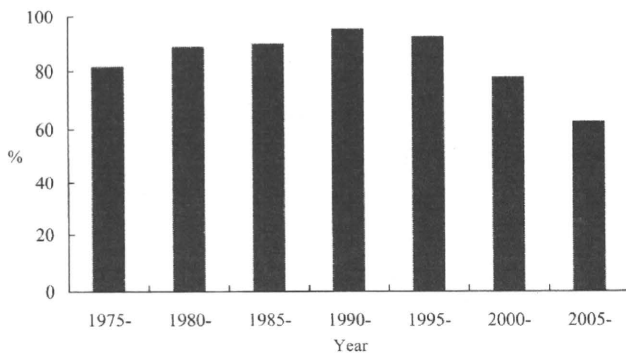


**Fig. 1** Transition of the preoperative pathological diagnostic rate

imaging, the detection rate for small pulmonary lesions with ground-glass opacity (GGO) in peripheral lung regions has increased. As a result, an increase in the complete resection of pathological stage IA non-small-cell lung cancer (NSCLC) has been suggested as a possibility for reducing lung cancer mortality.<sup>2-4</sup>

Although CT images show suspected lung cancer, the number of cases with a difficult preoperative pathological diagnosis has increased because these lesions are small and peripherally located. At the Niigata Cancer Center Hospital, the number of lung cancer patients who undergo pulmonary resection with a preoperative pathological diagnosis has decreased annually since 1990 (Fig. 1). Because of the increase in preoperatively undiagnosed surgical candidates, there is an increasing concern about such patients undergoing unnecessary diagnostic or therapeutic surgical interventions.

The aim of this retrospective study was to evaluate the diagnostic yield for preoperative CT imaging and the validity of diagnostic and therapeutic surgical intervention for suspected malignant pulmonary tumors based on the clinical decision of various experts.

### Patients and methods

We retrospectively reviewed 1755 patients who underwent pulmonary resection for histologically confirmed lung cancer or “strongly suspected” lung cancer between January 1999 and December 2007 (a thoracic radiologist has been on staff at our institution since 1999).

All patients underwent preoperative staging with CT scans to evaluate the lungs, pulmonary nodules, and mediastinum. CT scanning was performed with a single detector row scanner (High Speed Advantage; GE Medical System, Milwaukee, WI, USA), and 5 mm thick contiguous collimation was used to evaluate the entire lung. All primary tumors were evaluated with thin-section CT. Helical scans with a 1-mm collimation pitch were performed through the primary tumor. Intrave-

nous contrast material was routinely used. As the next step, bronchoscopy with fluoroscopy was performed to establish a histological diagnosis when the lesion could be recognized by X-rays or when the originating segment could be identified on CT images. When it was difficult to arrive at a pathological diagnosis by bronchoscopic cytology (or biopsy), a CT-guided needle biopsy or surgical intervention was considered depending on the nodule’s characteristics.

When the histological findings of “strongly suggestive of malignancy” or “conclusive for malignancy” were obtained by bronchoscopic cytology, sputum cytology, or CT-guided needle biopsy, they were defined as having “preoperatively histologically proven lung cancer (p/p lung cancer).” Patients for whom preoperative pathological findings were not obtained owing to the presence of small and/or peripherally located lesions were defined as having “suspected lung cancer (s/o lung cancer)” based on the preoperative CT imaging and clinical judgment at preoperative and postoperative joint conferences. The conferences comprised three board-certified respiratory surgeons, two trained surgeons, four board-certified respiratory physicians, two board-certified pathologists, one board-certified radiologist, and three well-trained cytotechnologists. We mainly assessed the indeterminate pulmonary nodules based on morphological features on CT images (shape, margin characteristics, size, density) and additionally evaluated the hemodynamic features depending on the lesion’s characteristics (especially for solid tumors).

Basic evaluations for s/o lung cancer lesions are as follows. In general, the presence of spicules, bronchus signs, vessel signs, visceral pleura retraction and thickening, older age ( $\geq 70$  years), lesions  $> 3$  cm in diameter, and clear imaging evidence are suggestive of malignancy.<sup>5,6</sup> Additional points of view that are held at our institution are as follows.

- GGO lesions: partly solid GGO lesions, GGO lesions without a shrinking tendency, and pure GGO lesions with pseudocavitation (small, focal, low-attenuation regions within or surrounding the periphery of a nodule) and internal air bronchograms are highly suggestive of bronchioloalveolar carcinoma (BAC).<sup>7,8</sup>
- Enhanced CT imaging: Enhancement of  $> 20$  Hounsfield units (HU) typically indicates malignancy.<sup>9-12</sup>
- clinical features: age, history of prior malignancy, presenting symptoms, and smoking history can be useful for suggesting a diagnosis.<sup>13,14</sup>

We comprehensively estimated the probability of malignancy for patients with s/o lung cancer based on the above radiological and clinical features.



The resected specimens were postoperatively evaluated in detail for criteria including the validity of clinical decision and compared to preoperative CT imaging. In cases in which surgery was performed without a preoperative diagnosis, the validity of the clinical decision for surgery was also evaluated.

The intraoperative algorithm for lesions that were pathologically undiagnosed preoperatively was as follows. First, brush cytology using a Tokyo Medical University (TMU) needle was performed. “Malignancy or suspected malignancy” was evaluated by two board-certified pathologists and three well-trained cytotechnologists.

If confirmed to be malignant, anatomical pulmonary resection with mediastinal lymph node dissection was essentially performed. If the lesion was not confirmed to be malignant, partial pulmonary resection including the whole lesion was performed, after which the resected specimen was evaluated using frozen sections. Depending on the frozen section results, surgical procedures with tumor-free margins were selected. For non-palpable lesions, a segmentectomy was performed depending on their CT location to avoid a positive surgical margin.

## Results

Following a diagnosis of lung cancer or suspected lung cancer, 1755 patients underwent pulmonary resection. Of the 1755 patients, 1107 were male (63.1%) and 648

were female (36.9%). The median age was 67.4 years (range 21–89 years). There were 1289 p/p lung cancer patients and 466 s/o lung cancer patients diagnosed using their CT images alone. Among the 1289 p/p lung cancer patients, the diagnosis was also confirmed postoperatively in 1282 patients, and 7 patients were definitively diagnosed with a noncancerous lesion. Among the 466 s/o lung cancer patients, 435 patients were definitely diagnosed with lung cancer, and 31 patients were diagnosed with noncancerous lesion.

The preoperative and intraoperative diagnostic procedures are shown in Table 1. Brush cytology using bronchoscopy was the most frequent preoperative diagnostic procedure. In all, 167 patients underwent pulmonary resection without pre- and intraoperative pathological diagnoses. The characteristics of s/o and p/p lung cancer patients are shown in Table 2. The number of patients with p-stage I disease was 383 (88.0%) in the s/o lung cancer group and 894 (69.7%) in the p/p lung cancer group ( $p < 0.01$ ). The numbers of patients with p-stage IA disease of adenocarcinoma  $\leq 2$  cm in diameter were 235 (54.0%) and 264 (20.6%) in the s/o and p/p lung cancer groups, respectively ( $p < 0.01$ ). There was no significant difference between the two groups for BAC with fibroblasts or non-BAC ( $p = 0.497$ ).

The lesions of the s/o lung cancer group were more likely to be located at peripheral sites than those of the p/p lung cancer group. Furthermore, lung cancers with GGO in the s/o lung cancer group contained either one of the radiological features described above.

**Table 1** Diagnostic procedures for patients who underwent pulmonary resection

Procedure	Lung cancer	No lung cancer
Total no. of patients	1717	38
Proven (p/p) lung cancer patients	1282	7
Preoperative diagnostic procedures		
Bronchoscopy with brush cytology	1029	5
CT-guided needle biopsy	220	2
Sputum cytology	33	0
Suspected (s/o) lung cancer patients	435	31
Intraoperative diagnostic procedures		
Needle biopsy using TMU needle	217	2
Partial resection	51	20
Undiagnosed or not performed	167	9

p/p, preoperatively histologically proven; s/o, suspected; TMU, Tokyo Medical University

**Table 2** Comparison between the s/o and p/p lung cancer groups

Parameter	s/o Lung cancer	p/p Lung cancer	<i>P</i>
Total no. of patients	435	1282	
p-Stage I	383 (88.0%)	894 (69.7%)	<0.01
p-Stage IA adenocarcinoma $\leq 2$ cm	235 (54.0%)	264 (20.6%)	<0.01
BAC with fibroblasts and non-BAC	275 (63.2%)	787 (61.4%)	0.497

BAC, bronchioloalveolar carcinoma

### Noncancerous lesions

A total of 38 noncancerous patients underwent pulmonary resection because of a preoperative diagnosis of lung cancer or suspected lung cancer. Seven of them were preoperatively misdiagnosed pathologically as having lung cancer. The definitive diagnoses for these lesions are shown in Table 3. There were two patients each with inflammatory pulmonary tumors and atypical adenomatous hyperplasia. Granuloma, tuberculoma, and sarcoma were seen in one patient each.

Altogether, 31 noncancer patients underwent pulmonary resection without a preoperative pathological diagnosis (Table 4). Inflammatory pulmonary tumors ( $n = 10$ ) were the most common pathology radiologically misdiagnosed as lung cancer.

**Table 3** Noncancerous lesions with preoperative pathological diagnosis of lung cancer ( $n = 7$ )

Lesion	No.
Inflammatory pulmonary tumor	2
Atypical adenomatous hyperplasia	2
Granuloma	1
Tuberculoma	1
Sarcoma	1

**Table 4** Noncancerous lesion without a preoperative pathological diagnosis ( $n = 31$ )

Lesion	No.
Inflammatory pulmonary tumor	10
Granuloma	4
Cryptococcoma	4
Amyloidoma	3
Hamartoma	2
Tuberculoma	2
Lymphoma	1
Others	5

### Diagnostic yield of CT imaging

Among the 1755 patients who underwent surgery, 1717 were definitively confirmed as having lung cancer; thus, the diagnostic yield of preoperative CT imaging was 97.8% (1717/1755). Furthermore, among the 466 s/o lung cancer patients, the results of 435 were found at surgery to be compatible with the predicted findings of lung cancer, and the diagnostic yield for surgical intervention was thus 93.3% (435/466) (Table 5).

### Discussion

Recent advances in CT imaging have increased the detection rate for peripherally located small pulmonary nodules. As shown in Table 2, the main factor contributing to the increase in the preoperative nondiagnostic rate was small adenocarcinomas recognized on CT.

Several studies, mainly focusing on the evaluation of morphological characteristics and on the differentiation between malignant and benign pulmonary lesions reported that the sensitivity, specificity, and accuracy of high-resolution and spiral CT techniques were 89%–94%, 57%–65%, and 79%–84%, respectively (Table 6).<sup>5,15,16</sup> Recent studies focusing on the hemodynamic characteristics of dynamic helical CT set the cutoff threshold at 15–30 HU and reported sensitivities of 81%–99%, specificities of 54%–93%, and accuracies of 77%–92% (Table 6).<sup>9–12,16</sup> The sensitivity was almost

**Table 5** Correspondence of the definitive diagnosis and preoperative pathological diagnosis

Preoperative pathological diagnosis	Definitive diagnosis		Total
	Lung cancer	No cancer	
Yes	1282	7	1289
No	435	31	466
Total	1717	38	1755

**Table 6** Diagnostic yields of CT based on morphological features and hemodynamic characteristics

Study	Year	Evaluation	No. of nodules	Sensitivity (%)	Specificity (%)	Accuracy (%)
Seemann <sup>15</sup>	1999	Morpho	104	91	57	84
Seemann <sup>5</sup>	2000	Morpho	104	89	61	83
Swensen <sup>9</sup>	2000	Hemody	356	98	58	77
Yi <sup>10</sup>	2004	Hemody	131	99	54	78
Jeong <sup>11</sup>	2005	Hemody	107	94	90	92
Yi <sup>12</sup>	2006	Hemody	119	81	93	85
Lee <sup>16</sup>	2007	Morpho and hemody	486	94* (89) [92]	65* (79) [79]	79* (84) [86]

Morpho, morphological features; Hemody, hemodynamic characteristics

\*Rate based on morphological features; ( ), rate based on hemodynamic characteristics; [ ], rate based on both morphological features and hemodynamic characteristics

equivalent to the evaluations of morphological features and hemodynamic characteristics. The specificity tended to be lower than that with the evaluation of hemodynamic characteristics. Furthermore, when both hemodynamic characteristics and morphological features were evaluated, the sensitivity, specificity, and accuracy were better than the evaluation by hemodynamic characteristics alone.<sup>12</sup>

Recently, there has been an increase in the number of studies investigating the differences between CT and other imaging modalities for evaluating solitary pulmonary nodules. Reports demonstrating the benefit of non-CT modalities are occasionally documented. However, a meta-analysis comparing representative imaging modalities—dynamic CT, dynamic magnetic resonance imaging (MRI), <sup>18</sup>F-fluorodeoxyglucose positron emission tomography (FDG-PET), <sup>99m</sup>Tc-depreotide single photon emission computed tomography (SPECT)—showed that there are no significant differences among these tests.<sup>17</sup> As described above, we believe that it is possible to evaluate solitary pulmonary nodules in detail using CT alone. Because we focused only on suspected malignant lesions, a sufficient evaluation could not be conducted for sensitivity, specificity, accuracy, or positive and negative predictive values, but 1717 of 1755 p/p lung cancer and s/o lung cancer patients (97.8%) were definitively diagnosed with lung cancer. Moreover, among the 466 s/o lung cancer patients who underwent surgical intervention based on CT findings and the clinical judgment of various experts, the results of 435 were compatible with the predicted findings of lung cancer (93.3%, 435/466). This diagnostic yield for pulmonary nodules without a preoperative diagnosis is acceptable.

If indeterminate pulmonary lesions detected by chest radiography and/or CT are not difficult to confirm pathologically, how do we pursue a diagnosis with no surgical procedure? Diagnostic procedures using flexible bronchoscopy (FB) (e.g., bronchial brushing, bronchial washing, transbronchial biopsy) are mainly pathological diagnostic modalities. A review in the American College of Chest Physicians (ACCP) clinical practice guidelines indicated that the sensitivity of FB was 78% for the diagnosis of peripheral lesions, although it was 88% for diagnosing central disease. Furthermore, the sensitivity was 34% for peripheral lesions <2 cm in diameter.<sup>18</sup>

Compensating for the shortcomings of FB, CT-guided transthoracic needle biopsy (CTNB) is almost established as an important alternative procedure to diagnose peripherally located pulmonary lesions that are not accessible by FB or not visible on radiographs. However, there are several fatal complications associated with CTNB including coronary and cerebral infarction due

to air embolism.<sup>19,20</sup> Pleural dissemination after CTNB has also been reported, despite the fact that lesions are recognized at an early stage of surgery.<sup>21,22</sup> Ost et al. and the ACCP evidence-based clinical practice guidelines recommend surgical resection for suspected malignant pulmonary nodules.<sup>14,23</sup> Considering the harm caused by CTNB, an invasive diagnostic procedure, its use at our institution has gradually decreased. It is performed in only a limited number of patients who do not desire surgery but who must undergo other treatments, such as chemotherapy and irradiation, based on histopathological features.

Surgical resection is the standard diagnostic procedure. The advantage of surgical intervention under general anesthesia is that it can be changed to oncological resection and include a lymphadenectomy based on the intraoperative pathological diagnosis during the same procedure. Intraoperative histopathological consultations have high diagnostic accuracy.<sup>24</sup> We also perform the same surgical intervention when we encounter suspected malignant and surgical candidates with a pulmonary lesion. In our study, the intraoperative diagnostic yield (needle biopsy using a TMU needle and partial resection) and the definitive diagnostic rate of lung cancer in patients without a preoperative pathological diagnosis were 61.6% (268/435) and 93.3% (435/466), respectively. We believe that the diagnostic yield by surgical resection for suspected lung cancer is high enough to be acceptable for suspected lung cancer patients. False-positive rates for patients who undergo pulmonary resection for lung cancer or suspected lung cancer are admissible.

Although the importance of preoperative pathological diagnosis remains highly valued, clinical judgment is also important as recommended by the ACCP clinical practice guidelines.<sup>14</sup> Patients with suspected malignant lesions benefit if doctors chose to perform a surgical intervention based on a well-considered radiographic evaluation and clinical judgment rather than taking an unnecessarily long time for a preoperative pathological diagnosis.

## Conclusion

Our study results showed that the diagnostic yields of CT imaging for lung cancer and suspected lung cancer, based on an evaluation from various experts, were sufficiently high. Furthermore, surgical diagnostic procedures are acceptable if the clinical probability of malignancy is high, including the above-listed radiological features, and the malignancy is pathologically undiagnosed.

## References

1. Statistics and Information Department, Minister's Secretariat, Ministry of Health, Labour and Welfare. Vital statistics of Japan 2007. No. 1, p. 296–301 (in Japanese).
2. Port JL, Kent MS, Korst RJ, Libby D, Pasmantier M, Altorki NK. Tumor size predicts survival within stage IA non-small cell lung cancer. *Chest* 2003;124:1828–33.
3. Wisnivesky JP, Yankelevitz D, Henschke CI. The effect of tumor size on curability of stage I non-small cell lung cancers. *Chest* 2004;126:761–5.
4. Birim O, Kappetein AP, Takkenberg JJ, van Klaveren RJ, Bogers AJ. Survival after pathological stage IA nonsmall cell lung cancer: tumor size matters. *Ann Thorac Surg* 2005;79:1137–41.
5. Seemann MD, Seemann O, Luboldt W, Bonel H, Sittek H, Dienemann H, et al. Differentiation of malignant from benign solitary pulmonary lesions using chest radiography, spiral CT and HRCT. *Lung Cancer* 2000;29:105–24.
6. Erasmus JJ, Connolly JE, McAdams HP, Roggli VL. Solitary pulmonary nodules. Part I. Morphologic evaluation for differentiation of benign and malignant lesions. *Radiographics* 2000;20:43–58.
7. Park CM, Goo JM, Lee HJ, Lee CH, Chun EJ, Im JG. Nodular ground-glass opacity at thin-section CT: histologic correlation and evaluation of change at follow-up. *Radiographics* 2007;27:391–408.
8. Oda S, Awai K, Liu D, Nakaura T, Yanaga Y, Nomori H, et al. Ground-glass opacities on thin-section helical CT: differentiation between bronchioloalveolar carcinoma and atypical adenomatous hyperplasia. *AJR Am J Roentgenol* 2008;190:1363–8.
9. Swensen SJ, Viggiano RW, Midthun DE, Muller NL, Sherrick A, Yamashita K, et al. Lung nodule enhancement at CT: multicenter study. *Radiology* 2000;214:73–80.
10. Yi CA, Lee KS, Kim EA, Han J, Kim H, Kwon OJ, et al. Solitary pulmonary nodules: dynamic enhanced multi-detector row CT study and comparison with vascular endothelial growth factor and microvessel density. *Radiology* 2004;233:191–9.
11. Jeong YJ, Lee KS, Jeong SY, Chung MJ, Shim SS, Kim H, et al. Solitary pulmonary nodule: characterization with combined wash-in and washout features at dynamic multi-detector row CT. *Radiology* 2005;237:675–83.
12. Yi CA, Lee KS, Kim BT, Choi JY, Kwon OJ, Kim H, et al. Tissue characterization of solitary pulmonary nodule: comparative study between helical dynamic CT and integrated PET/CT. *J Nucl Med* 2006;47:443–50.
13. Erasmus JJ, McAdams HP, Connolly JE. Solitary pulmonary nodules. Part II. Evaluation of the indeterminate nodule. *Radiographics* 2000;20:59–66.
14. Gould MK, Fletcher J, Iannettoni MD, Lynch WR, Midthun DE, Naidich DP, et al. Evaluation of patients with pulmonary nodules: when is it lung cancer? ACCP evidence-based clinical practice guidelines (2nd edition). *Chest* 2007;132(suppl):108S–30S.
15. Seemann MD, Staebler A, Beinert T, Dienemann H, Obst B, Matzko M, et al. Usefulness of morphological characteristics for the differentiation of benign from malignant solitary pulmonary lesions using HRCT. *Eur Radiol* 1999;9:409–17.
16. Lee KS, Yi CA, Jeong SY, Jeong YJ, Kim S, Chung MJ, et al. Solid or partly solid solitary pulmonary nodules: their characterization using contrast wash-in and morphologic features at helical CT. *Chest* 2007;131:1516–25.
17. Cronin P, Dwamena BA, Kelly AM, Carlos RC. Solitary pulmonary nodules: meta-analytic comparison of cross-sectional imaging modalities for diagnosis of malignancy. *Radiology* 2008;246:772–82.
18. Rivera MP, Mehta AC. Initial diagnosis of lung cancer: ACCP evidence-based clinical practice guidelines (2nd edition). *Chest* 2007;132(suppl):131S–48S.
19. Mokhlesi B, Ansaarie I, Bader M, Tareen M, Boatman J. Coronary artery air embolism complicating a CT-guided transthoracic needle biopsy of the lung. *Chest* 2002;121:993–6.
20. Tomiyama N, Yasuhara Y, Nakajima Y, Adachi S, Arai Y, Kusumoto M, et al. CT-guided needle biopsy of lung lesions: a survey of severe complication based on 9783 biopsies in Japan. *Eur J Radiol* 2006;59:60–4.
21. Kim JH, Kim YT, Lim HK, Kim YH, Sung SW. Management for chest wall implantation of non-small cell lung cancer after fine-needle aspiration biopsy. *Eur J Cardiothorac Surg* 2003;23:828–32.
22. Matsuguma H, Nakahara R, Kondo T, Kamiyama Y, Mori K, Yokoi K. Risk of pleural recurrence after needle biopsy in patients with resected early stage lung cancer. *Ann Thorac Surg* 2005;80:2026–31.
23. Ost D, Fein AM, Feinsilver SH. Clinical practice: the solitary pulmonary nodule. *N Engl J Med* 2003;348:2535–42.
24. Marchevsky AM, Changsri C, Gupta I, Fuller C, Houck W, McKenna RJ Jr. Frozen section diagnoses of small pulmonary nodules: accuracy and clinical implications. *Ann Thorac Surg* 2004;78:1755–9.